

Supplementary Information

Design of ligand mediated anisotropic Co₃O₄ nanorods for improved green hydrogen production electrochemically across different pH levels and substrates

Ariful Hoque^a, Shiv Kumar Patel^a, Harikrishnan K^a, Rajendra^a, Umesh K. Gaur^{b}, Manu Sharma^{a*}*

^aSchool of Nano Sciences, Central University of Gujarat, Gandhinagar, Gujarat

^bVP & RPTP Science College, Vallabh Vidya Nagar, India

**Corresponding author, Email: manu.sharma@cug.ac.in*

Electrochemical measurements:

The electrochemical measurements are done by a three-electrode system (Metrohm Autolab). The three-electrode half-cell consisted of one 3 mm glassy carbon (GC) and Ni foams as the working electrodes, 3M KCl saturated Ag/AgCl as the reference electrode, and a platinum wire as an auxiliary electrode. The working electrodes were designed by dispersion of 5 mg electrocatalyst in 250 μ L water and 250 μ L of isopropyl alcohol followed by adding 25 μ L of Nafion. The ink was sonicated for one hour to form a thick slurry. 3 μ L of the slurry was drop casted in the GCE followed by drying in an oven at 50 °C. For the Ni foam as a working electrode preparation, the foams were cut into 1 cm x 1 cm pieces and cleaned to remove hydroxide layers using 5% HCl solution followed by water and alcohol and dried the electrodes and drop casted over them (ex-situ working electrode fabrication). All the observed potentials were converted to reversible hydrogen electrode potential using the Nernst equation:

$$E_{RHE} = E_{Ag/AgCl} + 0.059 * pH + E_{Ag/AgCl}^0$$

$$E_{Ag/AgCl}^0 = 0.197 V \text{ at room temperature, } 0.5M H_2SO_4, pH = 0.3$$

The Tafel equation was used for the calculation of the Tafel slope (b)

$$\eta = b \log j + c$$

Here, 'b' is the Tafel slope, 'j' is the current density, 'η' is the overpotential, and 'c' is a constant. Tafel slopes are calculated from the kinetically controlled regions of the linear sweep voltammetry (LSV) polarization curves.

Table S1. The amount taken for the synthesis of different electrocatalysts

Electrocatalysts	$\text{Co}(\text{NO}_3)_2 \cdot 6\text{H}_2\text{O}$	$\text{C}_6\text{H}_9\text{NO}_6$	IPA	DDW	Temperature	Time
CO1	0.1 M	0.8 M	15	105	180 °C	12 h
CO2	0.1 M	0.8 M	15	105	180 °C	18 h
CO3	0.1 M	0.8 M	15	105	180 °C	24 h

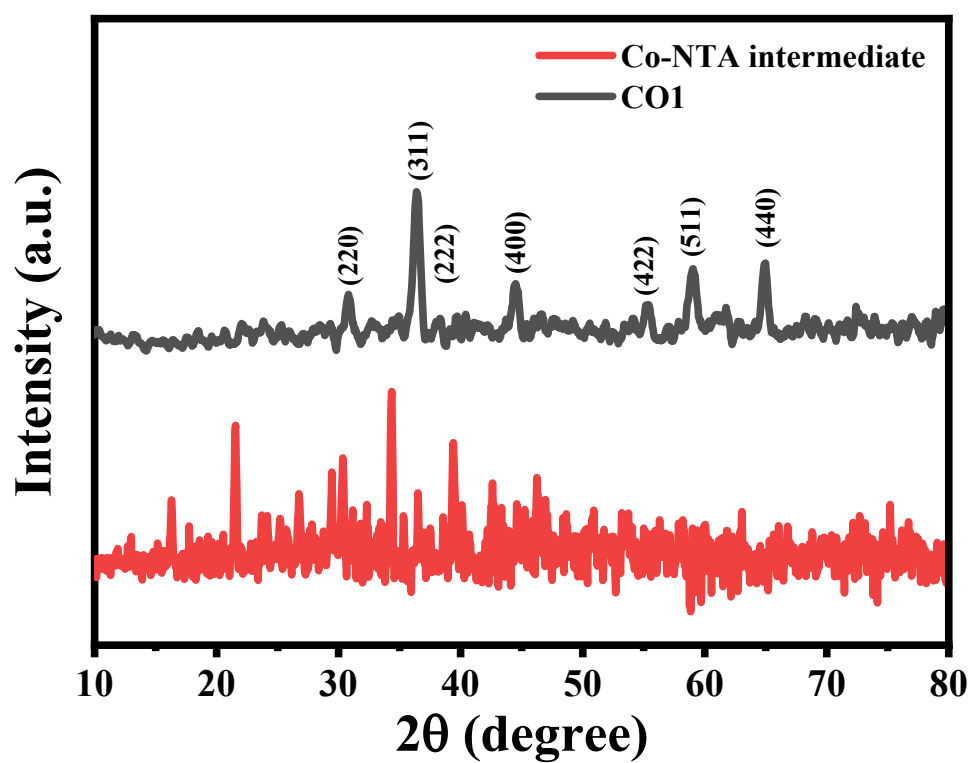


Figure S1. PXRD spectra of CO1 and Co-NTA intermediate complex.

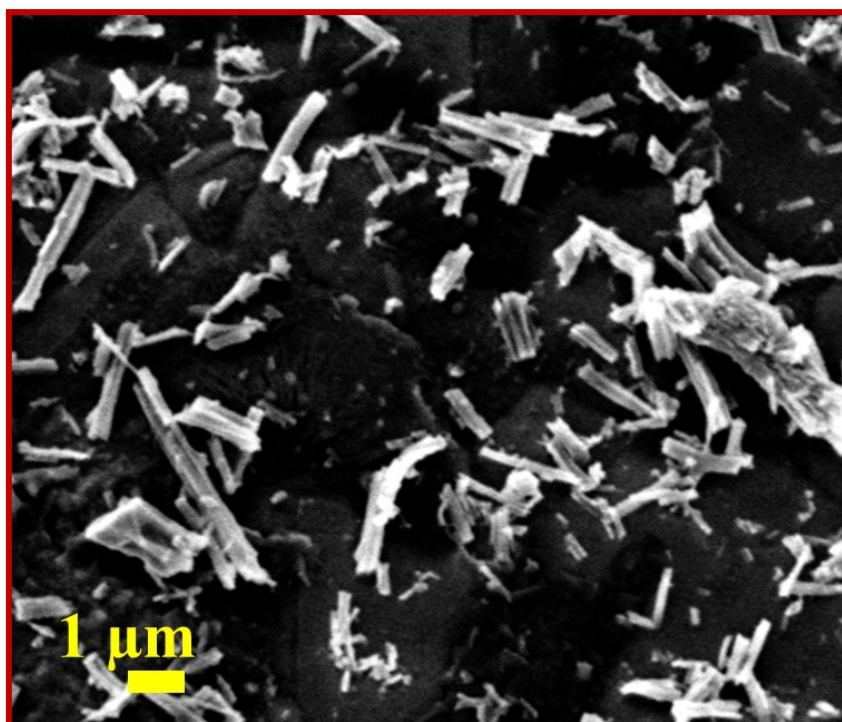


Figure S2. SEM image of CO1 with rodlike morphology.

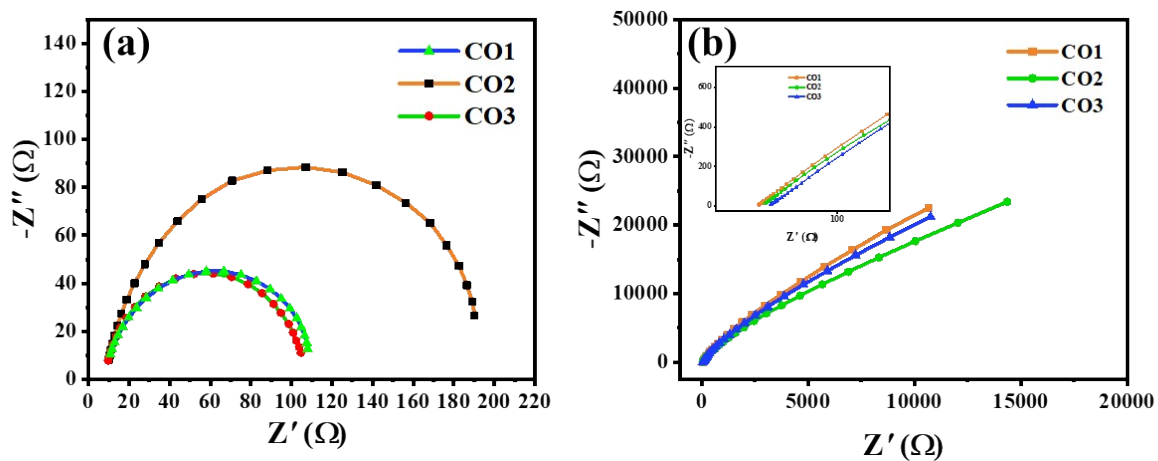


Figure S3. Nyquist plot of the electrocatalysts in (a) 0.5 M H_2SO_4 and (b) 1.0 M HClO_4 in GCE as a working electrode

Table S2. Summary of overpotentials and Tafel slopes of different electrocatalysts in GCE in 0.5 M H₂SO₄

Sl. No.	Electrocatalyst	Overpotential @ $\eta=10$ mA/cm ² (mV)	Tafel slope (mV/dec)	Charge transfer resistance, R _{CT} (ohm)
1	10 % Pt/C	82	119	-
2	CO1	724	155	97
3	CO2	759	208	180
4	CO3	828	139	94

Table S3. Summary of overpotentials and Tafel slopes of different electrocatalysts in GCE in 1.0 M HClO₄

Sl. No.	Electrocatalyst	Overpotential @ $\eta=10$ mA/cm ² (mV)	Tafel slope (mV/dec)
1	10 % Pt/C	209	309
2	CO1	815	71
3	CO2	858	93
4	CO3	904	104

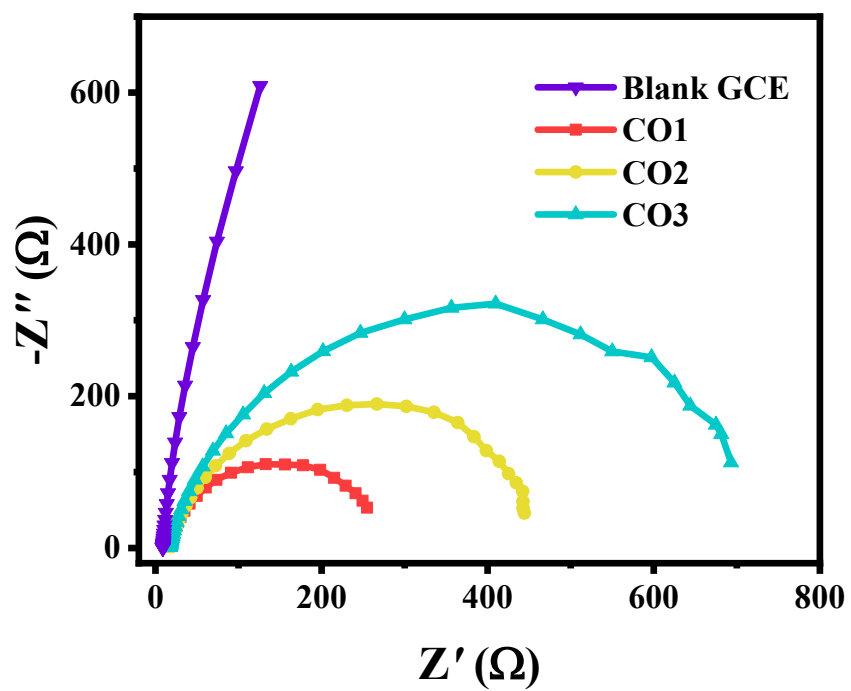


Figure S4. Nyquist plot of the electrocatalysts in 0.5 M KOH in GCE as working electrode.

Table S4. Summary of overpotentials, Tafel slopes, and charge transfer resistance (R_{CT}) of different electrocatalysts in GCE in 0.5 M KOH

Sl. No.	Electrocatalyst	Overpotential @ $\eta=10 \text{ mA/cm}^2$ (mV)	Tafel slope (mV/dec)	Charge transfer resistance, R_{CT} (ohm)
1	10 % Pt/C	210	300	
2	CO1	419	41	239
3	CO2	427	62	427
4	CO3	460	85	674

Table S5. Summary of overpotentials, Tafel slopes, and charge transfer resistance (R_{CT}) of different electrocatalysts in GCE in 1.0 M KOH

Sl. No.	Electrocatalyst	Mass loading (mg)	Overpotential @ $\eta=10$ mA/cm^2 (mV)	Tafel slope (mV/dec)	Charge transfer resistance (R_{CT}), ohm
1	10 % Pt/C	-	249	329	175
2	CO1	0.120	411	35	49
3	CO2	0.103	424	50	56
4	CO3	0.176	460	74	106

Table S6. Summary of overpotentials and Tafel slopes in Ni foam with different electrocatalyst loadings

Sl. No.	Electrocatalyst	Mass loading (mg)	Overpotential @ $\eta=10 \text{ mA/cm}^2$ (mV)	Tafel slope (mV/dec)
1	10% Pt/C		162	110
2	CO1 ₅₀	0.510	183	120
3	CO1 ₇₅	0.780	170	98
4	CO1 ₁₀₀	1.178	178	119

Exchange Current density¹:

Exchange current density is a crucial parameter in studying the intrinsic reactivity of the electrocatalysis process under equilibrium. The exchange current density is calculated from the Tafel equation when $\eta=0$. From the Tafel equation, the simplified expression is given as

$$i_{ex} = \frac{RT}{nFA\theta}$$

Where,

R is gas constant= $8.314 \text{ J K}^{-1} \text{ mol}^{-1}$

T is temperature= 298 K (the electrolysis was performed in room temperature)

n=2 (during HER the no of electrons involved is 2)

F is Faradays constant= 96485 C mol^{-1}

A is the area of the working electrode (=1 cm²)

θ is the resistance (R_{CT})

Table S7. Summary of R_{CT} and exchange current density for CO1 in Ni foam

Sl. No.	Electrocatalyst	R_s (ohm)	R_{CT} (ohm)	Exchange current density (A/cm ²)
1	CO1 ₅₀	0.92	6.67	0.00192
2	CO1 ₇₅	0.73	2.34	0.00548
3	CO1 ₁₀₀	0.78	6.45	0.00199

Electrochemical active surface area (ECSA):

The following expression calculates ECSA

$$ECSA(cm^2) = \frac{C_{dl}}{C_s}$$

Where, C_{dl} is the double-layer capacitance and was calculated from the non-faradic region (there is no charge transfer in this region). A linear fitting of the plot of the ΔJ vs scan rates calculates C_{dl} . The scan rates were taken as 20, 40, 60, 80, 100, and 120 mV/s. ' C_s ' is specific

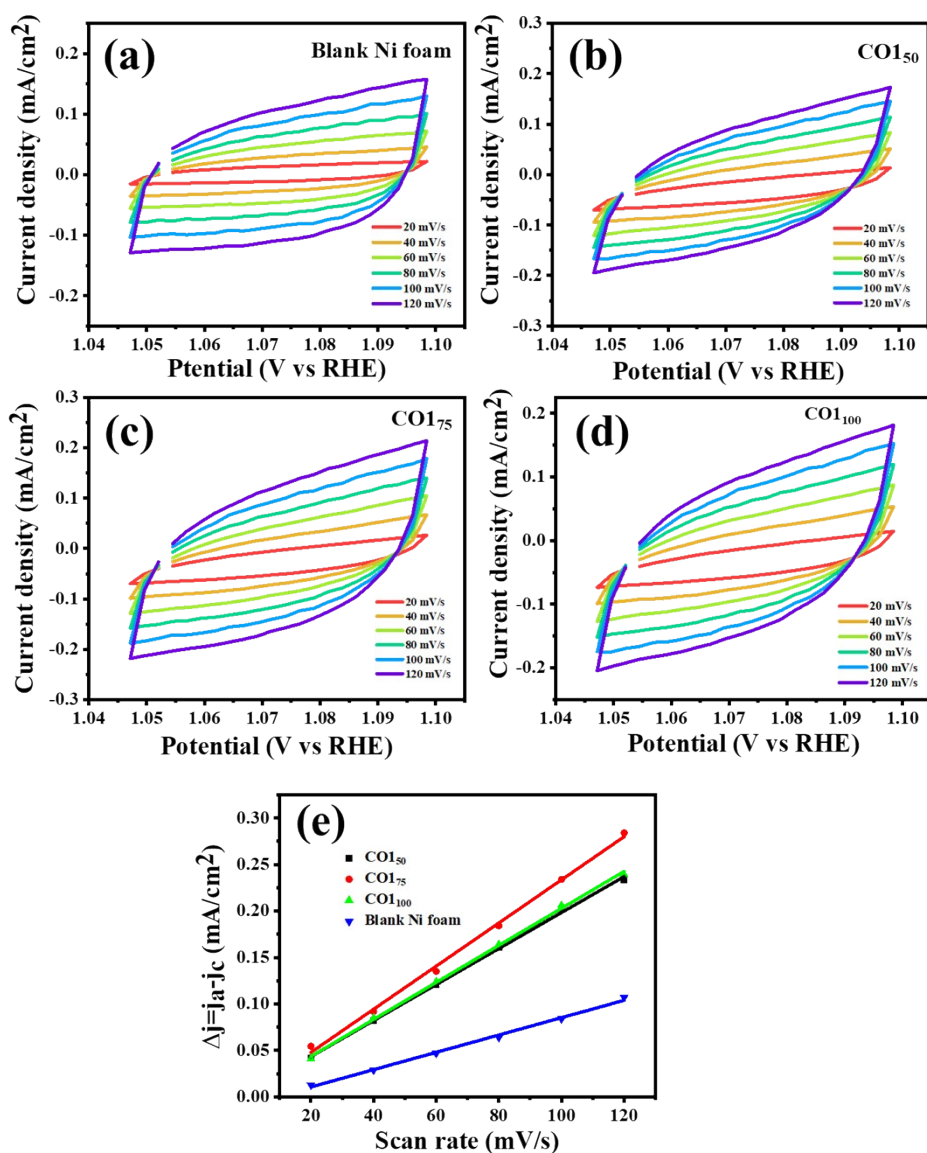


Figure S5. CV performed in a non-faradic region at different scan rates for (a) Blank Ni foam, (b) CO₁₅₀, (c) CO₁₇₅, (d) CO₁₁₀₀, and (e) is the current density vs scan rates for C_{dl} .

capacitance, C_s is Co is $27 \mu\text{F}/\text{cm}^2$ and for Ni is $40 \mu\text{F}/\text{cm}^2$ in alkaline media as reported in the previous report²⁻⁴.

Table S8. Brief of the double layer capacitance (C_{dl}) and Electrochemical active surface area (ECSA) of the CO1 electrocatalyst with different loadings.

Sl. No.	Electrocatalysts	Double layer capacitance (C_{dl} , mF)	ECSA (cm^2)
1	Blank Ni foam	1.92	23.27
2	CO1 ₅₀	1.94	71.85
3	CO1 ₇₅	2.32	85.92
4	CO1 ₁₀₀	1.99	73.70

Turnover frequency (TOF) ⁵:

In HER process, TOF quantifies the amount of produced hydrogen per active site per unit time. The TOF is calculated as

$$TOF = \frac{j.A}{2.F.m}$$

Here, j is the current density, A is the working electrode area, F is the Faradays constant, and m is the number of moles in the Co_3O_4 on the electrode. Now, substituting the values for TOF at $j@170 \text{ mV}$ for CO1₅₀= $5.4 \text{ mA}/\text{cm}^2$, CO1₅₀= $10 \text{ mA}/\text{cm}^2$, and CO1₅₀= $8.00 \text{ mA}/\text{cm}^2$ and geometrical area, $A=1 \text{ cm}^2$,

$$TOF = \frac{j.A}{2.F.m}$$

Table S9: Summary of the Concentration of the active sites and Turnover frequencies

Sl. No.	Electrocatalysts	Number of moles, m (mol*10 ⁻⁶)	Turnover frequency, TOF (s ⁻¹)
1	CO1 ₅₀	2.117	0.0132
2	CO1 ₇₅	3.239	0.0160
3	CO1 ₁₀₀	4.892	0.0085

Faradic efficiency (FE)^{6,7}:

The theoretical amount of produced gas can be calculated using Faraday's law of electrolysis with ideal gas law-

$$V_{\text{theoretical}} = \frac{RTQ}{npF}$$

Where, R and T are ideal gas constant and absolute temperature, Q is the charge at an applied current density of 20 mA/cm² for 100 minutes (6000 s), n is the number of electrons involved (for HER, n=2), p is the pressure and F is Faraday's constant.

The faraday's efficiency is calculated as the ratio between the experimental amount of produced hydrogen and theoretical amount of produced hydrogen-

$$FE = \frac{V_{\text{experimental}}}{V_{\text{theoretical}}}$$

V_{experimental} was measured by the inverted glass tube method and the faraday's efficiency is calculated as-

$$\begin{aligned} FE (\%) &= \frac{1.2 \text{ mL}}{1.52 \text{ mL}} \\ &= 78.94 \% \end{aligned}$$

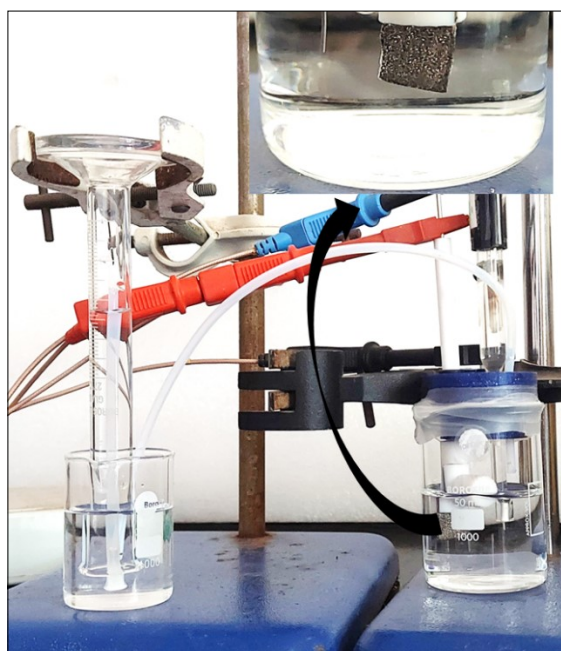


Figure S6. Inverted glass tube method for faradic efficiency estimation.

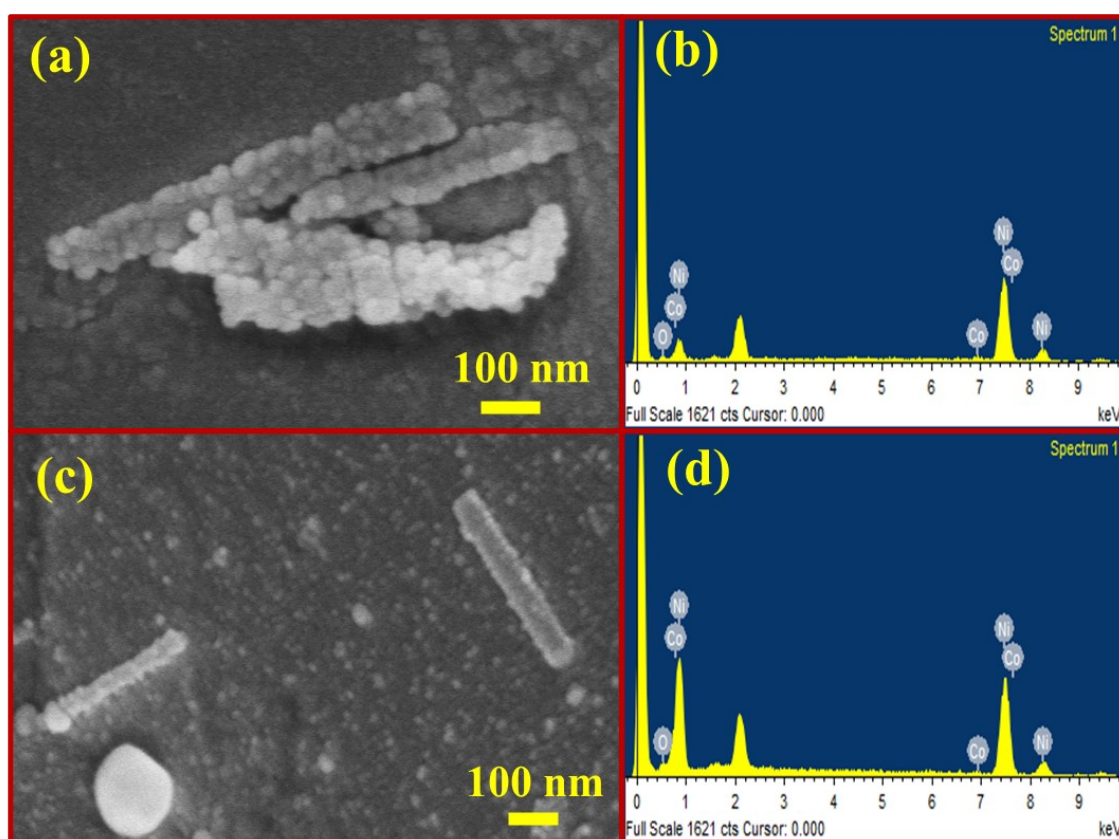


Figure S7. (a) & (b) FESEM and EDS of fresh CO1 drop casted in Ni foam, and (c) & (d) FESEM and EDS of CO1 after 24 h stability test.

Table S10. Comparison of HER activity of Co_3O_4 with others in literature, in a three-electrode system.

Sl. No.	Electrocatalyst	Electrolyte	WE Substrate	Overpotential @ 10	Tafel slope	Ref.
1	Layered Co_3O_4	1 M KOH	NiF	71	63	⁴
2	Co_3O_4 crystals	1 M KOH	NiF	195	50	⁸
3	Co_3O_4 nanoflower	1 M KOH	Carbon cloth	297	95.3	⁹
4	Co_3O_4 microtube	1 M KOH	NiF	190 @20	98	¹⁰
5	Co_3O_4 nanoplates	1 M KOH	ITO coated glass	523	71	¹¹
6	Urchin arrays of Co_3O_4	1 M KOH	NiF	225	53	¹²
7	Nanocrystals of Co_3O_4	1 M KOH	Carbon fiber paper	380	116	¹³
8	Co_3O_4 nanorod array	1 M KOH	GCE NiF	411 170	35 98	This work

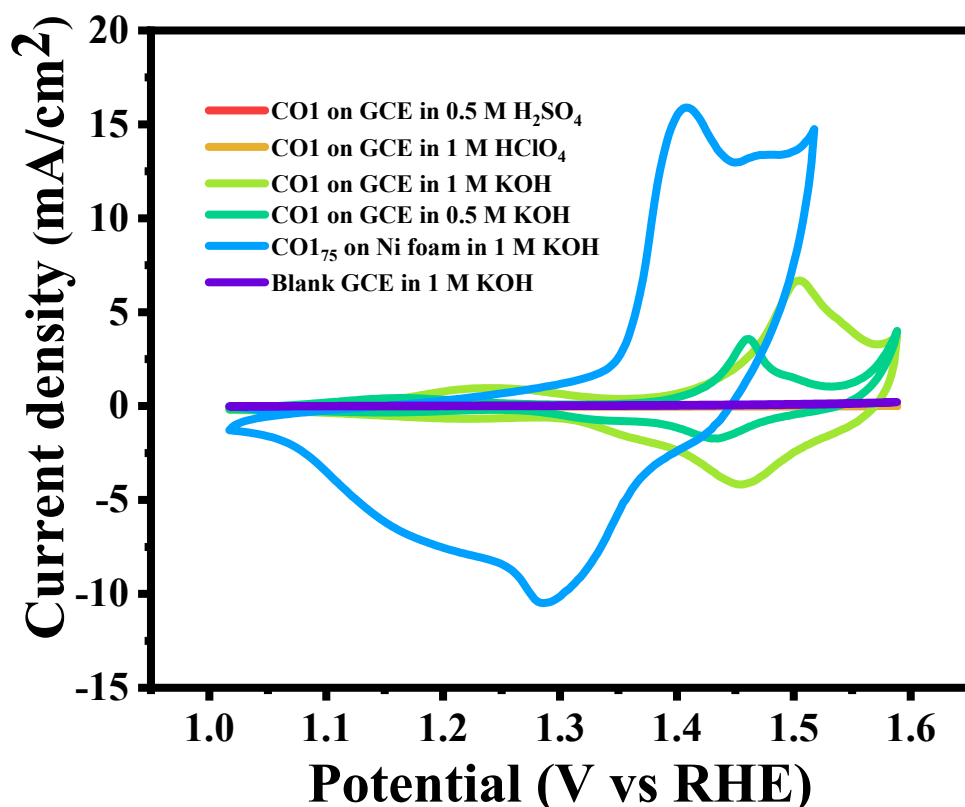


Figure S8. Cyclic voltammetry (CV) curves of CO1.

References

- (1) Chauhan, M.; Reddy, K. P.; Gopinath, C. S.; Deka, S. Copper Cobalt Sulfide Nanosheets Realizing a Promising Electrocatalytic Oxygen Evolution Reaction. *ACS Catal.* **2017**, *7* (9), 5871–5879. <https://doi.org/10.1021/acscatal.7b01831>.
- (2) Wu, G.; Li, N.; Zhou, D.-R.; Mitsuo, K.; Xu, B.-Q. Anodically Electrodeposited Co+Ni Mixed Oxide Electrode: Preparation and Electrocatalytic Activity for Oxygen Evolution in Alkaline Media. *Journal of Solid State Chemistry* **2004**, *177* (10), 3682–3692. <https://doi.org/10.1016/j.jssc.2004.06.027>.
- (3) McCrory, C. C. L.; Jung, S.; Peters, J. C.; Jaramillo, T. F. Benchmarking Heterogeneous Electrocatalysts for the Oxygen Evolution Reaction. *J. Am. Chem. Soc.* **2013**, *135* (45), 16977–16987. <https://doi.org/10.1021/ja407115p>.

- (4) Zhang, H.; Zhang, J.; Li, Y.; Jiang, H.; Jiang, H.; Li, C. Continuous Oxygen Vacancy Engineering of the Co₃O₄ Layer for an Enhanced Alkaline Electrocatalytic Hydrogen Evolution Reaction. *J. Mater. Chem. A* **2019**, *7* (22), 13506–13510. <https://doi.org/10.1039/C9TA03652K>.
- (5) Suryanto, B. H. R.; Wang, Y.; Hocking, R. K.; Adamson, W.; Zhao, C. Overall Electrochemical Splitting of Water at the Heterogeneous Interface of Nickel and Iron Oxide. *Nat Commun* **2019**, *10* (1), 5599. <https://doi.org/10.1038/s41467-019-13415-8>.
- (6) Urbain, F.; Smirnov, V.; Becker, J.-P.; Lambertz, A.; Yang, F.; Ziegler, J.; Kaiser, B.; Jaegermann, W.; Rau, U.; Finger, F. Multijunction Si Photocathodes with Tunable Photovoltages from 2.0 V to 2.8 V for Light Induced Water Splitting. *Energy Environ. Sci.* **2016**, *9* (1), 145–154. <https://doi.org/10.1039/C5EE02393A>.
- (7) Kumar, L.; Antil, B.; Kumar, A.; Das, M. R.; López-Estrada, O.; Siahrostami, S.; Deka, S. Experimental and Computational Insights into the Overall Water Splitting Reaction by the Fe–Co–Ni–P Electrocatalyst. *ACS Appl. Mater. Interfaces* **2023**, *15* (47), 54446–54457. <https://doi.org/10.1021/acsami.3c11947>.
- (8) Liu, L.; Jiang, Z.; Fang, L.; Xu, H.; Zhang, H.; Gu, X.; Wang, Y. Probing the Crystal Plane Effect of Co₃O₄ for Enhanced Electrocatalytic Performance toward Efficient Overall Water Splitting. *ACS Appl. Mater. Interfaces* **2017**, *9* (33), 27736–27744. <https://doi.org/10.1021/acsami.7b07793>.
- (9) Du, J.; Li, C.; Tang, Q. Oxygen Vacancies Enriched Co₃O₄ Nanoflowers with Single Layer Porous Structures for Water Splitting. *Electrochimica Acta* **2020**, *331*, 135456. <https://doi.org/10.1016/j.electacta.2019.135456>.
- (10) Zhu, Y. P.; Ma, T. Y.; Jaroniec, M.; Qiao, S. Z. Self-Templating Synthesis of Hollow Co₃O₄ Microtube Arrays for Highly Efficient Water Electrolysis. *Angewandte Chemie International Edition* **2017**, *56* (5), 1324–1328. <https://doi.org/10.1002/anie.201610413>.
- (11) Zhou, X.; Xia, Z.; Tian, Z.; Ma, Y.; Qu, Y. Ultrathin Porous Co₃O₄ Nanoplates as Highly Efficient Oxygen Evolution Catalysts. *J. Mater. Chem. A* **2015**, *3* (15), 8107–8114. <https://doi.org/10.1039/C4TA07214F>.
- (12) Li, R.; Zhou, D.; Luo, J.; Xu, W.; Li, J.; Li, S.; Cheng, P.; Yuan, D. The Urchin-like Sphere Arrays Co₃O₄ as a Bifunctional Catalyst for Hydrogen Evolution Reaction and Oxygen Evolution Reaction. *Journal of Power Sources* **2017**, *341*, 250–256. <https://doi.org/10.1016/j.jpowsour.2016.10.096>.

- (13) Du, S.; Ren, Z.; Zhang, J.; Wu, J.; Xi, W.; Zhu, J.; Fu, H. Co₃O₄ Nanocrystal Ink Printed on Carbon Fiber Paper as a Large-Area Electrode for Electrochemical Water Splitting. *Chem. Commun.* **2015**, *51* (38), 8066–8069. <https://doi.org/10.1039/C5CC01080B>.